EPR Study of $S = 2$ and $S = 3$ States of Fe−O−Fe Dimers in $Na_4[Fe(edta)]_2O\cdot 3H_2O$ and $\{[Fe(phen)_2]_2O\}(NO_3)_4\cdot 7H_2O$. X-ray Structure Determination of $Na_4[Fe(edta)]_2O\cdot 3H_2O$

Andrzej Ozarowski, Bruce R. McGarvey,* and John E. Drake

Department of Chemistry and Biochemistry, University of Windsor, Windsor, Ontario N9B 3P4, Canada

Received March 22, 1995[⊗]

X-band EPR single crystal studies have been done on two Fe−O−Fe dimers, $Na_4[Fe(edta)]_2O\cdot 3H_2O$ and $\{[Fe(phen)_2]_2O\}(NO_3)_4\cdot 7H_2O$, and the room-temperature X-ray structure of $Na_4[Fe(edta)]_2O\cdot 3H_2O$ was obtained. The compound crystallizes as monoclinic in the space group $P2_1/n$ (No. 14), having cell parameters $a = 16.08(1)$ Å, $b = 10.776(4)$ Å, $c = 18.367(8)$ Å, $\beta = 106.44(4)°$, $V = 3051(4)$ Å^3, and $Z = 4$; $R = 0.0490$, $R_w = 0.0369$. Resonances were identified by intensity variation with temperature for both the quintet ($S = 2$) and septet ($S = 3$) states of the dimer in both compounds and their spin-Hamiltonian parameters measured. A single resonance line for the triplet state was also observed in the phen complex in a limited range of orientations at a magnetic field near the limit of our magnet (15 kG). The zero-field-splitting (ZFS) parameters obtained were D_2, E_2, D_3, $E_3 = 0.248(1)$, $0.060(1)$, $0.604(1)$, $-0.016(1)$ cm^{-1} for the edta complex and $0.256(1)$, $0.037(1)$, $0.686(1)$, $-0.008(1)$ cm^{-1} for the phen complex. From these values, we can separate the contribution of the exchange parameter anisotropy from that due to local distortions of the ligand field near each Fe(III) ion. $|D_{exchange}|$, $|E_{exchange}| = 1.25$, 0.03 cm^{-1} for the edta complex and 1.41, 0.02 cm^{-1} for the phen complex, and in both complexes the z axis is parallel to the Fe−Fe axis. These values are surprisingly large, considering the theories presently used to explain the same effect in Cu−O−Cu dimers, and indicate that these theories need to be reexamined. Our results predict that $|D_1|$, $|E_1| = 3.00$, 0.62 cm^{-1} for the edta complex and 2.33, 0.31 cm^{-1} for the phen complex. Confirmation of these values will require EPR studies at frequencies greater than Q-band.

Introduction

Many transition metals form binuclear complex compounds in which the metal ions either interact directly or interact through non-metal bridging atoms. Such systems have been the subject of extensive investigations in coordination chemistry, particularly since their importance in biological systems has become known. A pair of copper atoms is found at the active site of hemocyanines in some mollusks,[1] the FeOFe core is found in cytochrome *c* oxidase and in hemerithrins that certain invertebrates use for oxygen transport,[2] and oxo-bridged manganese sites have been found in many enzymes,[3] to mention only a few examples. The metal−metal interactions in such systems affect their magnetic and EPR spectra.

Bihomonuclear complexes with one μ-oxo bridge can be formed from metal ions with electronic configurations d^1, d^2, d^3, d^4, and d^5. Those with d^1, d^3, and d^4 are found to be diamagnetic, and those with d^1, d^2, d^3, and d^4 are reported to be linear. The iron(III) (d^5) complexes generally have a bent structure with FeOFe angles in the range 130−175° although some recently reported iron(III) complexes[4] with bulky ligands have linear bridges. Molecular orbital calculations[5−7] have been applied to account for these observations with limited success.

The magnetic properties of the M−M dimers are usually interpreted in terms of the antiferromagnetic HDVV Hamiltonian

$$\mathcal{H} = J_{12}S_1\cdot S_2 \qquad (1)$$

where S_1 and S_2 are the spin operators of the interacting ions and J_{12} is the isotropic exchange integral between the ground state orbitals of the two metal ions. In this notation J_{12} is equal to the singlet−triplet separation and is positive for antiferromagnetic interactions. The Hamiltonian gives rise to a series of energy levels characterized by the total spin S that assumes values over the range $|S_1 - S_2|$ to $|S_1 + S_2|$, *i.e.* 0, 1, 2, 3, 4, and 5 for iron(III) compounds. J_{12} is found from magnetic susceptibility measurements to be about 200 cm^{-1} for μ-oxo Fe(III) complexes (except for some compounds with porphyrin ligands) and to be independent of bridging angle.[8] The lack of angular dependence is in striking contrast to the case of binuclear dihydroxo-bridged copper(II) compounds, where a very strong linear dependence of J_{12} upon the CuOCu bridging angle was found.[9]

Much less is known about the EPR of the FeOFe compounds. The only two papers dealing with EPR appeared over 20 years ago for $enH_2[Fe(hedta)]_2O\cdot 6H_2O$[10] and $Fe[(salen)]_2O\cdot CHCl_3$,[11] but no full interpretation of the EPR spectra were presented. It is interesting to note that no EPR spectrum was observed for the $Fe[(salen)]_2O\cdot CH_2Cl_2$ complex.[12a] Similar solvent effects were observed in other systems.[12b]

In this paper, we will report a detailed interpretation of the EPR spectra of two binuclear iron(II) complexes: $Na_4[Fe-$

* To whom all correspondence should be addressed.

[⊗] Abstract published in *Advance ACS Abstracts,* October 1, 1995.

(1) Solomon, E. I. *Struct. Bonding (Berlin)* **1983**, *53*, 1.
(2) Stenkamp, R. E.; Sieker, L. C.; Jensen, L. H. *J. Am. Chem. Soc.* **1984**, *106*, 618.
(3) Recent reviews: (a) Vincent, J. B.; Christou, G. *Adv. Inorg. Chem.* **1989**, *33*, 197. (b) Wieghardt, K. *Angew. Chem., Int. Ed. Engl.* **1989**, *28*, 1153. (c) *Bioinorganic Chemistry of Manganese*; Pecoraro, V. L., Ed.; VCH: New York, 1992.
(4) Buchanan, R. M.; O'Brien, R. J.; Richardson, J. F. *Inorg. Chim. Acta* **1993**, *214*, 33.
(5) Hay, P. J.; Thibeault, J. C. Hoffmann, R. *J. Am. Chem. Soc.* **1975**, *97*, 4884.
(6) Dunitz, J.; Orgel, L. E. *J. Chem. Soc.* **1953**, 2594.
(7) Jezowska-Trzebiatowska, B.; Wojciechowski, W. *Transition Met. Chem.* **1970**, *6*, 1.
(8) Murray, K. S. *Coord. Chem. Rev.* **1974**, *12*, 1.
(9) Hodgson, D. J. *Prog. Inorg. Chem.* **1975**, *19*, 173.
(10) Okamura, M. Y.; Hoffman, B. M. *J. Chem. Phys.* **1969**, *51*, 3128.
(11) Jezowska-Trzebiatowska, B.; Kozlowski, H.; Cukierda, T.; Ozarowski, A. *J. Mol. Struct.* **1973**, *19*, 663.
(12) (a) Coggon, P.; McPhail, A. T.; Mabbs, F. E.; McLachlan, V. N. *J. Chem. Soc. A* **1969**, 2850. (b) Ozarowski, A. Thesis, Department of Chemistry, Wroclaw University, 1978.

0020-1669/95/1334-5558$09.00/0

(edta)]$_2$O·3H$_2$O (**I**) (edta = ethylenediaminetetraacetate) and {[Fe(phen)$_2$]$_2$O}(NO$_3$)$_4$·7H$_2$O (**II**) (phen = 1,10-phenanthroline). Magnetic susceptibility measurements have yielded J_{12} = 198 cm^{-1} for **I**[13] and J_{12} = 220 cm^{-1} for **II**.[14] The crystal structure of **II** has been reported[15] as triclinic with the space group $P\bar{1}$ with a μ-oxo bridge angle of 155.1°. The X-ray structure determination for **I** is reported below.

Experimental Details

Synthesis of Na$_4$[Fe(edta)]$_2$O·3H$_2$O. Fe(OH)$_3$ was obtained by reacting solutions of ammonia and iron(III) chloride which was then purified by several decantations. A little less than stoichiometric amount of powdered disodium ethylenediaminetetraacetate was added and the mixture boiled for a few minutes until almost all of the solid Fe(OH)$_3$ had disappeared. Addition of dimethylformamide (DMF) to the deep-red hot filtered solution resulted in precipitation of the crude product, which was then redissolved in water (4 g in 20 mL). DMF was added dropwise to the hot solution until precipitation was about to commence. The solution was then placed in a thermostated bath at 60 °C until high-quality deep-red crystals suitable for X-ray investigation appeared after a few hours. After filtration, some small crystals were returned to the mother liquor which was kept at 60 °C until some crystals appropriate for EPR study were formed, about 2 × 2 × 2 mm in size. Note: Evaporation of aqueous solutions or precipitation by DMF at room temperature does not yield the same compound. The compound was originally reported to possess twelve water molecules,[13,16] but our X-ray study showed only three water molecules. The compound is hygroscopic and presumably may contain variable amounts of water in its powder form, depending on preparative and storage conditions.

Synthesis of {[Fe(phen)$_2$]$_2$O}(NO$_3$)$_4$·7H$_2$O. The compound was prepared as described in the literature[14,15,17] by reacting a slurry of 1,10-phenanthroline with an aqueous solution of iron(III) nitrate nonahydrate. Deep-red crystals were obtained by slow evaporation of an aqueous solution which was slightly acidified with nitric acid. Some solutions that were not acidified yielded an unidentified green compound that is thought from its EPR spectrum to be a monomeric iron complex.

EPR Spectra. The EPR spectra were recorded on a Bruker ESP-300e spectrometer equipped with an electromagnet capable of reaching 15 kG, an NMR magnetometer, a microwave counter, a variable-temperature accessory, and an accurate single-axis crystal rotator. Crystals of a size about 2 × 2 × 2 mm were used, and spectra were recorded every 2° over a 180° rotation. In addition to the powder spectra taken at X-band in this laboratory, powder spectra were recorded at 34, 3.9, and 2.4 GHz by Dr. Ralph Weber, Bruker Instruments, Billerica, MA. Intensities of selected resonances in the single-crystal spectra were measured at various temperatures to identify to which spin state they belonged. The spin-Hamiltonian parameters for the quintet ($S = 2$) and septet ($S = 3$) states were determined from the room-temperature single-crystal spectra.

Structure Determination and Refinement. Suitable crystals of Na$_4$[Fe(edta)]$_2$O·3H$_2$O were sealed in a capillary tube and mounted on a Rigaku AFC6S diffractometer with graphite-monochromated Mo Kα radiation.

Cell constants and an orientation matrix for data collection, obtained from a least-squares refinement using the setting angles of 25 carefully centered reflections in the range 22.94° < 2θ < 30.66° corresponded to a monoclinic cell, the dimensions being given in Table 1. On the basis of systematic absences of $h0l$, $h + l = 2n + 1$, and $0k0$, $k \neq 2n + 1$, and the successful solution and refinement of the structure, the space group was determined to be $P2_1/n$ (No. 14).

Table 1. Crystallographic Data for Na$_4$[Fe(edta)]$_2$O·3H$_2$O

chem formula	$C_{20}H_{30}O_{20}N_4Fe_2Na_4$	fw	850.12
a, Å	16.08(1)	T, °C	23
b, Å	10.776(4)	λ, Å	0.710 69
c, Å	18.367(8)	ρ_{calcd}, g cm^{-3}	1.85
β, deg	106.44(4)	μ, cm^{-1}	10.96
V, Å^3	3051(4)	abs range	0.94−1.00
space group	$P2_1/n$ (No. 14)	R^a	0.0490
Z	4	$R_w{}^b$	0.0369
		GoF	1.68

$^a R = \sum||F_o| - |F_c||/\sum|F_o|$. $^b R_w = [(\sum w(|F_o| - |F_c|)^2/\sum wF_o^2)]^{1/2}$.

The data were collected at a temperature of 23 ± 1 °C using the ω−2θ scan technique to a maximum 2θ value of 50.0°. The ω scans of several intense reflections, made prior to data collection, had an average width at half-height of 0.36° with a takeoff angle of 6.0°. Scans of (1.37 + 0.30 tan θ)° were made at a speed of 32.0°/min (in ω). The weak reflections ($I < 10.0\sigma(I)$) were rescanned (maximum of two rescans), and the counts were accumulated to ensure good counting statistics. Stationary-background counts were recorded on each side of the reflection. The ratio of peak counting time to background counting time was 2:1. The diameter of the incident beam collimator was 0.5 mm, and the crystal to detector distance was 250.0 mm.

Of the 5906 reflections which were collected, 5693 were unique (R_{int} = 0.126). The intensities of the three representative reflections which were measured after every 150 reflections remained constant throughout data collection, indicating crystal and electronic stability (no decay correction was applied).

The linear absorption coefficient for Mo Kα is 11.0 cm^{-1}. An empirical absorption correction, based on azimuthal scans of several reflections, was applied, which resulted in transmission factors ranging from 0.94 to 1.00. The data were corrected for Lorentz and polarization effects.

The positions of the iron atoms were obtained from sharpened Patterson synthesis, and the positions of the remaining non-hydrogen atoms were determined from subsequent difference Fourier maps.[18] The non-hydrogen atoms, with the exception of the carbon atoms, were treated anisotropically, and the hydrogen atoms were included in their idealized positions with C−H set at 0.95 Å and with isotropic thermal parameters set at 1.2 times that of the carbon atom to which each was attached. The final cycle of the full-matrix least-squares refinement[19] was based on 2098 observed reflections ($I > 3.00\sigma(I)$) and 316 variable parameters and converged (largest parameter shift was 0.001 times its esd) with unweighted and weighted agreement factors of

$$R = \sum||F_o| - |F_c||/\sum|F_o| = 0.0490$$

$$R_w = [(\sum w(|F_o| - |F_c|)^2)/(\sum wF_o^2)]^{1/2} = 0.0369$$

The standard deviation of an observation of unit weight[20] was 1.68. The weighting scheme was based on counting statistics and included a factor (p = 0.03) to downweight the intense reflections. Plots of $\sum w(|F_o| - |F_c|)^2$ versus $|F_o|$, reflection order in data collection, (sin θ)/λ, and various classes of indices showed no unusual trends. The maximum and minimum peaks on the final difference Fourier map corresponded to +0.52 and −0.39 e/Å^3, respectively.

(13) Schugar, H.; Rossman, G. R.; Barraclough, C. G.; Gray, H. B. *J. Am. Chem. Soc.* **1972**, *94*, 2683.
(14) Khedekar, A. V.; Lewis, J.; Mabbs, F. E.; Weigold, H. J. *J. Chem. Soc. A* **1967**, 1561.
(15) Plowman, J. E.; Loehr, T. M.; Schauer, C. K.; Anderson, O. P. *Inorg. Chem.* **1984**, *23*, 3553.
(16) Schugar, H.; Walling, C.; Jones, R. B.; Gray, H. B. *J. Am. Chem. Soc.* **1967**, *89*, 3712.
(17) Gaines, A.; Hammett, L. P.; Walden, G. H., Jr. *J. Am. Chem. Soc.* **1936**, *58*, 1668.
(18) Structure solution methods: Calbrese, J. C. PHASE—Patterson Heavy Atom Solution Extractor. Ph.D. Thesis, University of Wisconsin—Madison, 1972. Beurskens, P. T. DIRDIF: Direct Methods for Difference Structures—an automatic procedure for phase extension and refinement of difference structure factors. Technical Report 1984/1; Crystallography Laboratory: Toernooiveld, 6525 Ed Nijmegen, The Netherlands, 1984.
(19) Least-squares: Function minimized $\sum w(|F_o| - |E_c|)^2$, where $w = F_o^2\sigma(F_o^2)$, $\sigma^2(F_o) = [S^2(C + R^2B) + (pF_o^2)]/(Lp)^2$, S = scan rate, C = total integrated peak count, R = ratio of scan time to background counting time, B = background count, Lp = Lorentz−polarization factor, and p = p factor.
(20) Standard deviation of an observation of unit weight: $[\sum w(|F_o| - |F_c|)^2/(N_o - N_v)]^{1/2}$, where N_o = number of observations and N_v = number of variables.

Table 2. Final Fractional Coordinates and B(eq) Values for Non-Hydrogen Atoms of $Na_4[Fe(edta)]_2O\cdot 3H_2O$ with Standard Deviations in Parentheses

atom	x	y	z	B(eq), Å^2
Fe(1)	0.57411(6)	0.3408(1)	0.73802(5)	1.41(4)
Fe(2)	0.39294(6)	0.1531(1)	0.73096(5)	1.24(4)
Na(1)	0.4446(2)	−0.1470(3)	0.5036(2)	2.8(1)
Na(2)	0.2746(2)	0.1969(3)	1.0088(2)	2.8(1)
Na(3)	0.7370(2)	0.1598(3)	1.0107(2)	2.5(1)
Na(4)	0.5005(2)	−0.3225(3)	0.9539(2)	3.8(2)
O(1)	0.4751(3)	0.2668(5)	0.7363(3)	2.1(2)
O(2)	0.6049(3)	0.2471(4)	0.6536(3)	2.2(2)
O(3)	0.7025(3)	0.2062(4)	0.5932(3)	2.5(2)
O(4)	0.6603(3)	0.2569(4)	0.8254(3)	2.0(2)
O(5)	0.7773(3)	0.2903(5)	0.9239(3)	2.6(2)
O(6)	0.5644(3)	0.4786(4)	0.8142(2)	1.9(2)
O(7)	0.4746(3)	0.6298(5)	0.8261(3)	2.6(2)
O(8)	0.3220(3)	0.5133(5)	0.5075(3)	2.4(2)
O(9)	0.4293(3)	0.6511(5)	0.5366(3)	3.1(2)
O(10)	0.3527(3)	0.2208(4)	0.8178(3)	1.8(2)
O(11)	0.2572(3)	0.2109(5)	0.8841(3)	3.1(3)
O(12)	0.2916(3)	0.2166(4)	0.6422(2)	1.6(2)
O(13)	0.1668(3)	0.1677(5)	0.5580(3)	2.9(2)
O(14)	0.4227(3)	0.0324(4)	0.6584(2)	1.8(2)
O(15)	0.5140(3)	−0.1146(5)	0.6443(3)	2.9(3)
O(16)	0.5758(3)	−0.1416(5)	0.9313(3)	3.1(2)
O(17)	0.6282(3)	0.0251(5)	0.9989(3)	3.6(3)
O(18)	0.4189(3)	0.0783(5)	0.5090(3)	2.5(2)
O(19)	−0.0237(3)	0.1302(5)	0.4199(3)	2.9(2)
O(20)	−0.1447(3)	0.0739(5)	0.5312(3)	3.5(3)
N(1)	0.6998(4)	0.4330(5)	0.7395(3)	1.6(2)
N(2)	0.5222(3)	0.4971(5)	0.6599(3)	1.4(2)
N(3)	0.2858(4)	0.0218(5)	0.7310(3)	1.5(2)
N(4)	0.4680(3)	0.0083(5)	0.8113(3)	1.2(2)
C(1)	0.6767(5)	0.2631(7)	0.6405(4)	1.7(1)
C(2)	0.7381(5)	0.3612(7)	0.6878(4)	2.2(2)
C(3)	0.7287(5)	0.3162(6)	0.8595(4)	1.6(1)
C(4)	0.7527(5)	0.4289(7)	0.8180(4)	1.9(2)
C(5)	0.6760(4)	0.5596(7)	0.7088(4)	1.8(1)
C(6)	0.5979(5)	0.5556(7)	0.6412(4)	1.8(1)
C(7)	0.5085(5)	0.5638(7)	0.7885(4)	1.7(1)
C(8)	0.4824(4)	0.5855(7)	0.7030(4)	1.9(1)
C(9)	0.3971(5)	0.5486(7)	0.5417(4)	1.7(1)
C(10)	0.4541(5)	0.4503(7)	0.5924(4)	2.1(2)
C(11)	0.2870(5)	0.1756(7)	0.8337(4)	1.8(1)
C(12)	0.2384(5)	0.0722(7)	0.7830(4)	2.1(2)
C(13)	0.2279(5)	0.1447(7)	0.6148(4)	1.9(1)
C(14)	0.2295(5)	0.0181(7)	0.6525(4)	2.3(2)
C(15)	0.3272(4)	−0.0988(7)	0.7577(4)	1.7(1)
C(16)	0.4033(4)	−0.0794(7)	0.8268(4)	1.6(1)
C(17)	0.4843(5)	−0.0468(7)	0.6830(4)	1.8(1)
C(18)	0.5247(4)	−0.0497(7)	0.7699(4)	1.9(1)
C(19)	0.5798(5)	−0.0267(7)	0.9422(4)	2.1(2)
C(20)	0.5218(5)	0.0614(6)	0.8847(4)	1.7(1)

Neutral-atom scattering factors were taken from Cromer and Waber.[21] Anomalous dispersion effects were included in F_c;[22] the values for $\Delta f'$ and $\Delta f''$ were those of Cromer.[23] All calculations were performed using the TEXSAN[24] crystallographic software package of the Molecular Structure Corp.

Results

Structure of $Na_4[Fe(edta)]_2O\cdot 3H_2O$. Final atomic coordinates for non-hydrogen atoms are given in Table 2, important distances and bond angles are given in Table 3, and an ORTEP diagram is given in Figure 1, illustrating the environment of Fe in the anion. The coordination polyhedron around each iron in the binuclear $[(edta)FeOFe(edta)]^{4-}$ anion approximates to a distorted octahedron with the bridging oxygen atom approximately trans to one of the nitrogen atoms of the edta group (with slight deviation from linearity (174.9(2) and 179.5(2)°). The FeOFe bond angle is 163.2(3)°. The arrangement is very similar to that reported for an oxygen-bridged binuclear iron(III) complex[25] formed with *N*-hydroxyethylenediaminetriacetate (hedta), namely $[(hedta)FeOFe(hedta)]^{2-}$, in which the deviation from linearity was slightly greater. Thus three of the tetraacetate groups have one of their oxygen atoms involved in coordination while the fourth is turned away from the iron atom at the center. The three oxygen atoms and one nitrogen atom essentially form

Table 3. Interatomic Distances (Å) and Important Angles (deg) for $Na_4[Fe(edta)]_2O\cdot 3H_2O$[a]

Fe(1)−O(1)	1.772(5)	Fe(2)−O(1)	1.784(5)
Fe(1)−O(2)	2.025(5)	Fe(2)−O(10)	2.019(5)
Fe(1)−O(4)	2.014(5)	Fe(2)−O(12)	2.068(5)
Fe(1)−O(6)	2.076(5)	Fe(2)−O(14)	2.014(5)
Fe(1)−N(1)	2.245(6)	Fe(2)−N(3)	2.230(6)
Fe(1)−N(2)	2.216(6)	Fe(2)−N(4)	2.250(6)
O(2)−C(1)	1.258(8)	O(10)−C(11)	1.270(8)
O(3)−C(1)	1.227(8)	O(11)−C(11)	1.217(8)
O(4)−C(3)	1.274(8)	O(12)−C(13)	1.270(8)
O(5)−C(3)	1.250(8)	O(13)−C(13)	1.239(7)
O(6)−C(7)	1.279(8)	O(14)−C(17)	1.289(8)
O(7)−C(7)	1.222(8)	O(15)−C(17)	1.208(8)
O(8)−C(9)	1.253(8)	O(16)−C(19)	1.253(9)
O(8)−C(9)	1.234(8)	O(17)−C(19)	1.242(8)
N(1)−C(2)	1.488(8)	N(3)−C(12)	1.483(8)
N(1)−C(4)	1.451(8)	N(3)−C(14)	1.470(8)
N(1)−C(5)	1.484(8)	N(3)−C(15)	1.479(8)
N(2)−C(6)	1.493(8)	N(4)−C(16)	1.492(8)
N(2)−C(8)	1.493(8)	N(4)−C(18)	1.481(8)
N(2)−C(10)	1.491(8)	N(4)−C(20)	1.495(8)
C(1)−C(2)	1.536(9)	C(11)−C(12)	1.519(9)
C(3)−C(4)	1.541(9)	C(13)−C(14)	1.53(1)
C(5)−C(6)	1.4496(9)	C(15)−C(16)	1.507(9)
C(7)−C(8)	1.524(9)	C(17)−C(18)	1.543(9)
C(9)−C(10)	1.531(9)	C(19)−C(20)	1.526(9)
Na(1)--O(9)[b]	2.291(6)	Na(3)--O(12)[c]	2.679(5)
Na(1)--O(18)	2.389(6)	Na(1)--O(18)[d]	2.470(6)
Na(4)--O(19)[e]	2.298(6)	Na(4)--O(20)[e]	2.517(7)
Fe(1)−O(1)−Fe(2)	163.2(3)		
O(1)−Fe(1)−O(2)	100.0(2)	O(1)−Fe(2)−O(10)	96.1(5)
O(1)−Fe(1)−O(4)	102.9(2)	O(1)−Fe(2)−O(12)	102.8(2)
O(1)−Fe(1)−O(6)	95.5(2)	O(1)−Fe(2)−O(14)	99.7(2)
O(1)−Fe(1)−N(1)	179.5(2)	O(1)−Fe(2)−N(3)	174.9(2)
O(1)−Fe(1)−N(2)	99.1(2)	O(1)−Fe(2)−N(4)	100.9(2)
O(2)−Fe(1)−O(4)	97.1(1)	O(10)−Fe(2)−O(12)	98.4(2)
O(2)−Fe(1)−O(6)	162.5(2)	O(10)−Fe(2)−O(14)	160.9(2)
O(2)−Fe(1)−N(1)	79.4(2)	O(10)−Fe(2)−N(3)	79.0(2)
O(2)−Fe(1)−N(2)	90.7(2)	O(10)−Fe(2)−N(4)	88.0(2)
O(4)−Fe(1)−O(6)	87.1(2)	O(12)−Fe(2)−O(14)	88.5(2)
O(4)−Fe(1)−N(1)	77.0(2)	O(12)−Fe(2)−N(3)	76.9(2)
O(4)−Fe(1)−N(2)	154.8(2)	O(12)−Fe(2)−N(4)	154.6(2)
O(6)−Fe(1)−N(1)	85.1(2)	O(14)−Fe(2)−N(3)	85.3(2)
O(6)−Fe(1)−N(2)	78.8(2)	O(14)−Fe(2)−N(4)	78.6(2)
N(1)−Fe(1)−N(2)	81.0(2)	N(3)−Fe(2)−N(4)	80.2(2)
Fe(1)−O(2)−C(1)	121.0(5)	Fe(2)−O(10)−C(11)	121.1(5)
Fe(1)−O(4)−C(3)	118.1(4)	Fe(2)−O(12)−C(13)	118.5(5)
Fe(1)−O(6)−C(7)	116.3(4)	Fe(2)−O(14)−C(17)	119.9(5)
Fe(1)−N(1)−C(2)	107.2(4)	Fe(2)−N(3)−C(12)	107.8(4)
Fe(1)−N(1)−C(4)	105.7(4)	Fe(2)−N(3)−C(14)	106.1(4)
Fe(1)−N(1)−C(5)	105.6(4)	Fe(2)−N(3)−C(15)	106.4(4)
Fe(1)−N(2)−C(6)	106.7(4)	Fe(2)−N(4)−C(16)	106.9(4)
Fe(1)−N(2)−C(8)	106.3(4)	Fe(2)−N(4)−C(18)	104.5(4)
Fe(1)−N(2)−C(10)	109.5(4)	Fe(2)−N(4)−C(20)	113.1(4)

[a] Only angles involving the Fe cores are listed. [b] $x, 1-y, z$. [c] $1/2+x, 1/2-y, 1/2+z$. [d] $1-x, y, 1-z$. [e] $1/2-x, y-1/2, 3/2-z$.

(21) Cromer, D. T.; Waber, J. T. *International Tables for X-ray Crystallography*; The Kynoch Press: Birmingham, England, 1974; Vol. IV, Table 2.2A.
(22) Ibers, J. A.; Hamilton, W. C. *Acta Crystallogr.* **1964**, *17*, 781.
(23) Cromer, D. T. *International Tables for X-ray Crystallography*; The Kynoch Press: Birmingham, England, 1974; Table 2.3.1.
(24) *TEXSAN-TEXRAY Structure Analysis Package*; Molecular Structure Corp.: The Woodlands, TX, 1985.
(25) Lippard, S. J.; Schugar, H.; Walling, C. *Inorg. Chem.* **1967**, *6*, 1825.

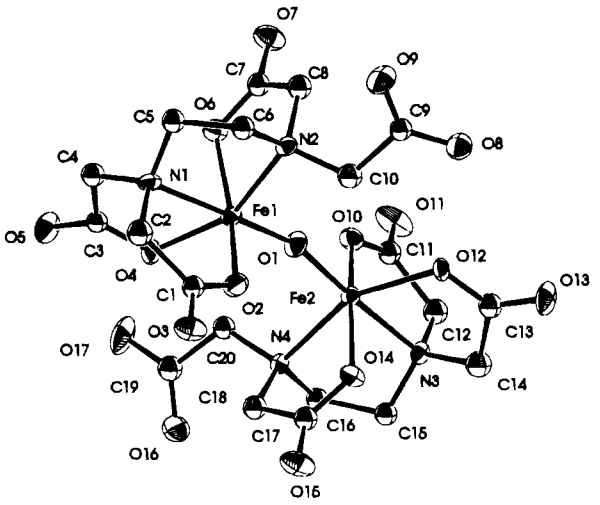

Figure 1. ORTEP diagram for anion in $Na_4[Fe(edta)]_2O{\cdot}3H_2O$.

a plane with the two iron atoms displaced by an average of 0.35 Å compared to 0.36 Å in the hedta complex.[25] There is no obvious pattern in the Fe−O bond lengths in this plane relative to their positions to the nitrogen atom. The average Fe−O (acetate) bond distance is 2.04(3) Å, which is considerably longer than the average Fe−O (bridge) bond distance of 1.778(8) Å. These distances are essentially identical to those observed in the hedta complex[25] as is the average of the Fe−N bond distance of 2.24(3) Å.

The average C−N distances for different environments within the ligands are not significantly different, but as with the hedta complex, the distances are such that the C−N bonds in the glycinate rings at 1.473(17) Å are shorter than those in the ethylenediamine rings at 1.487(7) Å and those attached to acetate groups not involved in complexing to iron at 1.493(2) Å. The reverse is the case for C−C bonds with C−C (glycinate) at 1.53(2) Å and C−C (ethylenediamine) at 1.502(5) Å. With acetate groups coordinated to iron, the average of the C−O (coordinated) bond length of 1.271(1) Å is longer that of the C−O (uncoordinated) bond length of 1.23(2) Å. The fourth acetate in each edta group ion, which is not bonded to iron, has an average C−O bond length of 1.246(9) Å, close to the average value for those in the coordinated acetate groups of 1.25(2) Å.

The environment about the sodium cations is interesting to note in that three of them are five-coordinated to oxygen atoms and one is four-coordinated with Na−O distances ranging from 2.291(6) Å for Na(1) to O(9), an oxygen atom in the acetate group not coordinated to iron, to 2.679(5) Å for Na(3) to O(12), an oxygen atom directly bonded to iron. The three water molecules are all associated with a sodium cation site. Na(1) has two close contacts with symmetry-related H_2O molecules with Na(1)−O(18) distances of 2.389(6) and 2.470(6) Å, while the other two water molecules are both associated with Na(4), with Na(4)−O(19) at 2.298(6) Å and Na(4)−O(20) at 2.517(7) Å.

EPR of $Na_4[Fe(edta)]_2O{\cdot}3H_2O$. Since we have only a single rotation axis goniometer and limited access to the X-ray crystallography apparatus, it was not possible to orient the crystals in the spectrometer using X-ray analysis. In the case of this crystal, we used the symmetry between the two magnetically inequivalent sites in the unit cell and crystal habit to fix the location of the crystal axes. The crystals grew with two types of prominent faces, and when the crystal was mounted with one type of face perpendicular to the rotation axis, we obtained the spectral behavior shown in Figure 2. For monoclinic symmetry, this behavior is expected only if the *b* axis is in the plane perpendicular to the rotation axis. The slight difference in the maximum heights, for the two magnetically inequivalent sites, results from the rotation axis being slightly off the perpendicular (1.6°). The crystal face thus had to be either the (100) plane or the (001) plane. Measurement of the angles in the rhombohedral face established that the face was in the (001) plane (the other prominent faces in the crystal were in the (111) planes) and also told us which of the two crossover points in Figure 2 was the *b* axis and which was the *a* axis. The axis of rotation then had to be close to the crystal c^* axis (the axis perpendicular to the *ab* plane). The spectra recorded for rotations about other crystallographic axes were very cluttered and more difficult to analyze but were useful in confirming our final spin-Hamiltonian assignments. The most striking feature is the absence of any resonances that could be attributed to the first excited state, a triplet with $S = 1$ lying 198 cm^{-1} above the singlet ground state. Intensity measurements showed that the strong resonances are due to the $S = 2$ state while some of the weak ones are due to $S = 3$ and the other ones are forbidden transitions within the $S = 2$ manifold. The orientation dependence for both the $S = 2$ and $S = 3$ transitions are shown in Figure 2. There are indications of the presence of resonances from the $S = 4$ state, but they are too weak to study their angular dependence or temperature dependencies.

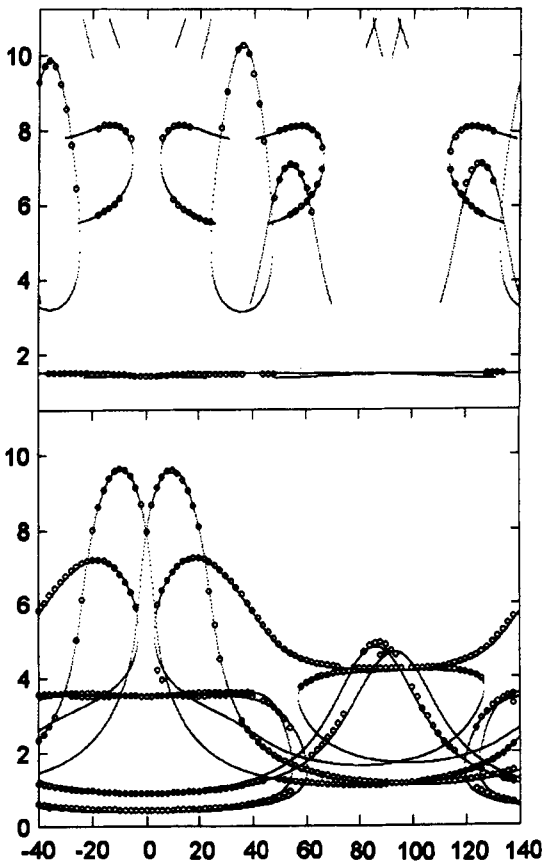

Figure 2. Plots of resonance fields identified as $S = 2$ and $S = 3$ resonances (top plot for $S = 3$) for a rotation axis close to the c^* axis of $Na_4[Fe(edta)]_2O{\cdot}3H_2O$. Experimental points are open circles, and dotted lines are calculated every 0.2° from best fit spin-Hamiltonian parameters. The abscissa is in angular degress with 0° being approximately the *a* axis. The ordinate is the magnetic field in kG.

EPR of $\{[Fe(phen)_2]_2O\}(NO_3)_4{\cdot}7H_2O$. The EPR spectra for one rotation are shown in Figure 3. The resonances were narrower than those for the edta complex, and since there was

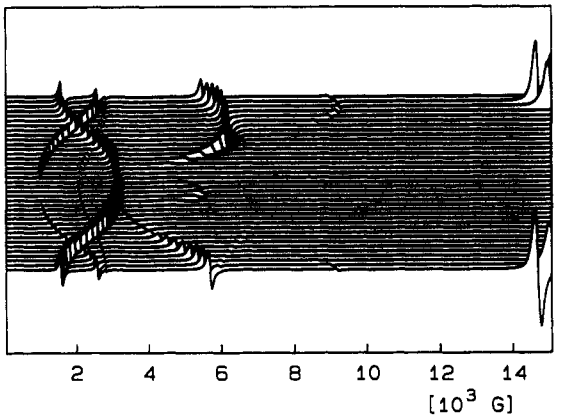

Figure 3. EPR spectra of $\{[Fe(phen)_2]_2O\}(NO_3)_4 \cdot 7H_2O$ taken every 5° in the rotation plane in which the $S = 1$ resonance was found. The $S = 1$ resonance is the large peak seen at magnetic fields above 14 kG.

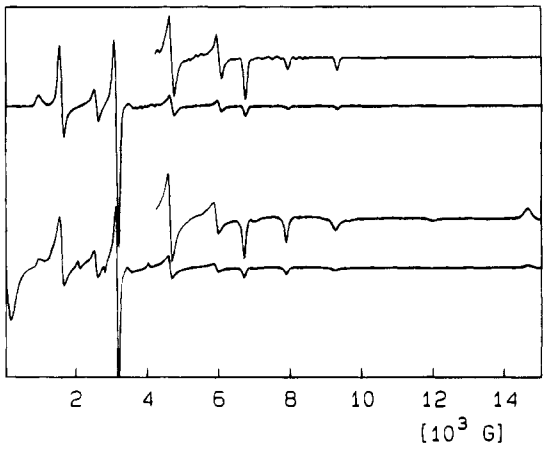

Figure 4. EPR at room temperature of powdered $\{[Fe(phen)_2]_2O\}(NO_3)_4 \cdot 7H_2O$. The upper spectrum is the simulated spectrum calculated for the $S = 2$ resonances, and the lower is the experimental spectrum.

only one magnetic site in the triclinic unit cell, the spectra were much clearer than were the spectra for the edta compound, allowing us to obtain spectra for three orthogonal rotation planes. Since we had no means to determine the location of the crystallographic axes relative to the laboratory axes, our spin-Hamiltonian results are reported only in terms of the principal axes. As for the edta complex, transitions within the quintet and septet states were observed. A very strong line appeared in one rotation plane over a very limited range of angles (see Figure 3) close to the upper limit of magnetic field available to us that, subsequent analysis revealed, could not belong to the quintet or septet states. The minimal resonance field for that transition was about 14.6 kG. Unfortunately, when the crystal was placed in the variable-temperature accessory, the resonance moved to higher magnetic fields due to the lowering of the klystron frequency from 9.8 to 9.4 GHz. Since the resonance moved to higher fields and moved beyond 15 kG as the temperature was lowered, we could not confirm that this resonance came from a transition within the triplet ($S = 1$) state, but the high-intensity resonance could be due to nothing else. Apparently the failure to detect the triplet state comes from its having a very large zero-field splitting, ZFS. This resonance is also seen in the high-field region of the powder spectrum (see Figure 4) where its amplitude is low due to a strong orientation dependence for the transition.

Spin-Hamiltonian Parameters. We have fitted the results to the spin-Hamiltonian

$$\mathcal{H} = \beta\, \mathbf{B}\cdot\mathbf{g}\cdot\mathbf{S} + D[S_z^2 - (1/3)S(S+1)] + E[S_x^2 - S_y^2] + B_4^0 O_4^0 + B_4^2 O_4^2 + B_4^4 O_4^4 \quad (2)$$

where $\mathbf{S}$ is the total spin operator in the system ($\mathbf{S} = \mathbf{S}_1 + \mathbf{S}_2$). The fourth-order spin operators were used in the standard form.[26] Incidentally, we found that all off-diagonal matrix elements of the spin-Hamiltonian for $S = 2$, expressed in terms of the a and F parameters, that are given in a review by Bencini and Gatteschi[27] are wrong. A least-squares method based on the SIMPLEX algorithm was developed to find the spin-Hamiltonian parameters. The function

$$f = \sum_i [h(\text{calc})_i - h(\text{expt})_i]^2 \quad (3)$$

where h are the resonance fields observed or calculated for a crystal rotation, was minimized with respect to the D, E, and quartic parameters. The large angular dependence of the spectra made misalignments of less than a degree significant, so we included the angles Θ and Φ, defining the orientation of the rotation axis versus the principal-axis system, as parameters in the minimization. The $\mathbf{g}$ matrix was assumed to be isotropic and equal to 2, as is generally found for high-spin Fe(III), because we found that any attempt to allow changes in $\mathbf{g}$ did not improve the fit. We also included the third-order HS^3 terms in the beginning, but the program consistently found very small values for the parameters without any improvement in the fit. The evaluation of resonance fields from assumed spin-Hamiltonian parameters required the diagonalization of complex 5×5 matrices for $S = 2$ and 7×7 matrices for $S = 3$, and this diagonalization was done using the Householder method.[28] We used an in-house program written in Microsoft Quick Basic 4.5. Calculation of all resonance fields and transition probabilities within $S = 2$ for one orientation of a crystal over a magnetic field range of 0−15 kG required about 1 s on a 80486DX/2-66 computer. Spin-Hamiltonian parameters obtained for the $S = 2$ and the $S = 3$ states for both compounds are given in Table 4. Powder spectra for $S = 2$ were simulated for both compounds using a related program and ZFS parameters from Table 4.

The two magnetic sites in the monoclinic edta complex allowed us to fix the a and b axes and therefore to locate the principal axes relative to the crystal axes and then relative to the molecular axes which, in turn, allowed us to measure the deviation of the principal axes of the ZFS matrix from the "expected" system of axes for the Fe−O−Fe unit (see Figure 5). The $S = 3$ system's principal axes are close to those given in Figure 5 with the main ZFS distortion axis in the z direction in the figure, namely, the Fe−Fe direction, but the principal axes for the $S = 2$ system are very different from those of the $S = 3$ system and appear to be unrelated to the assumed axes. This will be considered in detail below.

For the phen complex, location of the principal axes relative to the crystal system could not be determined. Unlike the situation for the edta system, we found in this case that all principal axes for both the $S = 2$ and the $S = 3$ systems were identical in their orientation. This also will be considered in more detail below.

Theoretical Analysis of D and E Parameters

Separation of Contributions. There are three contributions to the ZFS parameters found for a given spin state of an

(26) Abragam, A.; Bleaney, B. *Electron Spin Resonance of Transition Ions*; Clarendon Press: London, 1970.
(27) Bencini, A.; Gatteschi, D. *Transition Metal Chemistry*; Melson, G. A., Figgis, B. N., Eds.; Marcel Dekker: New York, 1982; Vol. 8, p 1.
(28) Wilkinson, J. H. *The Algebraic Eigenvalue Problem*; Clarendon Press: London, 1970.

Table 4. Spin-Hamiltonian Parameters[a]

compound	S	D	E	B_4^0	B_4^2	B_4^4
$Na_4[Fe(edta)]_2O{\cdot}3H_2O$	2	0.2477	0.0598	1.3	−2.9	31.4
	3	0.6044	−0.0158	−0.9	1.1	0.3
$[Fe(phen)_2]_2O(NO_3)_4{\cdot}7H_2O$	2	0.2562	0.0372	4.0	0.5	−1.8
	3	0.6863	−0.0079	−0.3	0.3	0.9

[a] Signs are relative not absolute. D and E are given in cm^{-1}, and B_n^m terms are given in 10^{-4} cm^{-1}. Errors are estimated to be $\pm 5 \times 10^{-4}$ cm^{-1} for D, E and $\pm 0.5 \times 10^{-4}$ cm^{-1} for B_n^m terms.

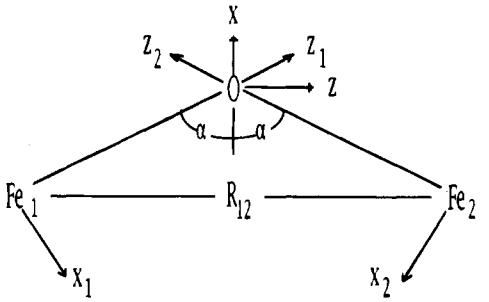

Figure 5. Location of the principal axes in the FeOFe dimer and definition of the angle α. The y axis is perpendicular to the FeOFe plane of the dimer. The subscripted axes are the principal axes of the individual ion's zero-field splitting that were assumed in the analysis.

exchange-coupled dimer. The point dipole magnetic interaction is an anisotropic $S_1{\cdot}D{\cdot}S_2$ interaction that gives rise to a contribution labeled D_{dipole} and E_{dipole}, while an anisotropy in the exchange interaction would give rise to terms of the form

$$D_{exchange} = J_{zz} - 0.5(J_{xx} + J_{yy}) \quad (4)$$

$$E_{exchange} = 0.5(J_{xx} - J_{yy}) \quad (5)$$

A third contribution comes into play when S_1, $S_2 > {}^1/_2$ because each individual ion will have a zero-field splitting caused by local distortions of the crystal field about each metal ion in the dimer. We will label this contribution by D_c and E_c. All three contributions are defined in terms of the individual spins S_1 and S_2 but our spin-Hamiltonians are defined in terms of the total spin S for a given state. The conversion between the two quantizations has been done[29] using the two parameters α_S and β_S:

$$D = \alpha_S D_e + \beta_S D_c = \alpha_S(D_{exchange} + D_{dipole}) + \beta_S D_c \quad (6)$$

$$E = \alpha_S E_e + \beta_S E_c = \alpha_S(E_{exchange} + E_{dipole}) + \beta_S E_c \quad (7)$$

$$\alpha_S = [S(S+1) + 2S_1(S_1+1) + 2S_2(S_2+1)]/[2(2S-1)(2S+3)] \quad (8)$$

$$\beta_S = [3S(S+1) - 3 - 2S_1(S_1+1) - 2S_2(S_2+1)]/[(2S-1)(2S+3)] \quad (9)$$

The different coefficients are required because two terms are of type $(S_1{\cdot}D{\cdot}S_2)$ and the third is of type $(S_1{\cdot}D_1{\cdot}S_1 + S_2{\cdot}D_2{\cdot}S_2)$. The conversion equations above assumed that the principal axes for all spin states S were identical in orientation. Since this was not the case in our edta complex, we will have to generalize them to apply to the **D** matrix in the general $\mathbf{S}{\cdot}D{\cdot}\mathbf{S}$ ZFS Hamiltonian operator. In this case eqs 6 and 7 can be generalized as

$$\mathbf{D}_{ij} = \alpha_S \mathbf{D}_{ij}^{e} + \beta_S \mathbf{D}_{ij}^{c} \quad (10)$$

The **D** matrix for the $S = 2$ system in the edta complex is given as follows in the a, b, c^* coordinate system for one of the magnetic sites in the unit cell:

a	−1339	277	395
b	277	824	−896
c^*	395	−896	515

where the elements are given in units of 10^{-4} cm^{-1}. The other can be obtained by a C_2 rotation about the b axis. The two matrices for the $S = 3$ system for the two magnetic sites **I** and **II** are

	I			**II**		
a	2019	−2792	21	1973	2807	33
b	−2792	154	−28	2807	200	11
c^*	21	−28	−2172	33	11	−2172

We give both matrices for $S = 3$ because we have no way of knowing which one is associated with the $S = 2$ matrix above and must consider both combinations in our analysis. Further, since absolute signs are not known, we need also to consider the case where matrices for $S = 3$ are of the opposite sign relative to the $S = 2$ matrix, giving us four combinations to consider. There are, of course, really eight combinations because all our sign assignments could be reversed, but this will simply change all the signs of the quantities determined in the first four combinations. We will see below that all these combinations will produce very similar results, so that our conclusions will be firmer than all these combinations would seem to suggest. We will use eq 10 to generate the two matrices $\mathbf{D}_{ij}^{e}$ and $\mathbf{D}_{ij}^{c}$ from the $S = 2$ matrix above and one of the $S = 3$ matrices above. The four possible combinations will be labeled as cases 1−4, which are defined as follows:

case 1: $S = 2$ matrix with $S = 3$ matrix **I** with signs as given above

case 2: $S = 2$ matrix with $S = 3$ matrix **I** of opposite signs

case 3: $S = 2$ matrix with $S = 3$ matrix **II** with signs as given above

case 4: $S = 2$ matrix with $S = 3$ matrix **II** of opposite signs

The individual matrices of $\mathbf{D}_{ij}^{e}$ and $\mathbf{D}_{ij}^{c}$ were then diagonalized to obtain D_e, E_e and D_c, E_c as well as the orientation of the principal axes for each matrix. Values of D_e, E_e and D_c, E_c are given in Table 5.

For D_e, E_e of all four cases, the principal axes align very well with the molecular axes shown in Figure 5 for one or the other of the two Fe−O−Fe units. Cases 1 and 2 line up with one unit, and cases 3 and 4, with the other, the main distortion axis, z, for all four cases, being no more than 3° from the z axis of Figure 5, the Fe−Fe direction. For cases 1 and 3 the x axis of the ZFS is close to the x axis of Figure 5 and the y axis of the ZFS is close to the y axis of Figure 5. In case 1 the angle is 2°, and for case 3 the angle is 9°. For cases 2 and 4 the x axis of the ZFS is close to the y axis of Figure 5 while the y axis is close to the x axis. The angles are 3° for case 4 and 17° for case 2. For the D_c, E_c matrix the major distortion axis, z, is also near the z axis of Figure 5. For cases 1 and 3 it makes an angle of only 4° with the Fe−Fe direction, and for cases 2 and

(29) Owen, J. *J. Appl. Phys.* **1961**, *32*, 213S.

Table 5. ZFS Parameters[a] for Different Cases

case	D_e	E_e	D_c	E_c	$D(1)$	$E(1)$
			$Na_4[Fe(edta)]_2O\cdot 3H_2O$			
1	±1.281	±0.035	±1.461	±0.116	∓4.677	∓0.683
		$D_{exchange}$, $E_{exchange}$ = 1.400, 0.035 or −1.162, −0.035				
2	∓1.256	±0.034	∓1.168	±0.111	±3.0001	∓0.620
		$D_{exchange}$, $E_{exchange}$ = −1.136, 0.034 or 1.375, −0.034				
3	±1.273	±0.037	±1.384	±0.096	∓4.298	∓0.537
		$D_{exchange}$, $E_{exchange}$ = 1.392, 0.037 or −1.154, −0.037				
4	∓1.263	±0.030	∓1.275	±0.050	±3.722	±0.281
		$D_{exchange}$, $E_{exchange}$ = −1.144, 0.030 or 1.383, −0.030				
			$[Fe(phen)_2]_2O(NO_3)_4\cdot 7H_2O$			
1	±1.415	∓0.020	±1.181	∓0.060	∓2.325	±0.308
		$D_{exchange}$, $E_{exchange}$ = 1.537, −0.020 or −1.293, 0.020				
2	∓1.465	±0.013	∓1.771	∓0.026	±5.911	±0.213
		$D_{exchange}$, $E_{exchange}$ = −1.343, 0.013 or 1.587, −0.013				

[a] All quantities are in cm^{-1}. See text for definitions of parameters.

4 the angle is 7°. For cases 1 and 2 the ZFS x axis is rotated away from the y axis of Figure 5 by 28° while for cases 3 and 4 the rotation angle is about 45°. Since the principal axes of D_c, E_c are determined by the ZFS interactions at the two Fe^{3+} centers, there is no reason to expect these axes to conform to those of Figure 5. It is apparent, however, that the main distortion at each site is due to the bridging oxygen.

For the phen complex, we do not know the relation of the principal axes in the crystal coordinate system, but the edta results would strongly suggest that the principal distortion axis of the ZFS interaction would also be the Fe−Fe direction and we have chosen to assume this is true in our analysis. Since this system was found to have the same principal axis for both the $S = 2$ and $S = 3$ states, we can use eqs 6 and 7 instead of eq 10 to extract values of D_e, E_e and D_c, E_c, which are given also in Table 5. Case 1 uses the relative signs for $S = 2$ and $S = 3$ states given in Table 4, and Case 2 reverses the sign for the S = 3 state. Analysis of the X-ray structure shows that the x axis in Figure 5 is very close to being a C_2 axis for the phen complex even though this is not required by the crystal symmetry; thus it seems reasonable to expect this to be one of the principal axes along with the Fe−Fe direction and this would require the D_c, E_c matrix along with the D_e, E_e matrix to have the principal axes shown in Figure 5.

It will be noted in Table 5 that the magnitudes for D_e, E_e do not differ much for the various combinations that had to be considered in the analysis. To a lesser extent, this is even true for the D_c, E_c values. Examination of eqs 8 and 9 will reveal that D and E for the $S = 3$ transitions are primarily due to D_e and E_e because β_3 (=−2/45) is an order of magnitude smaller than α_3 (=47/90), and therefore the values and principal axes for D and E of this spin state are essentially those of the D_e and E_e contribution. This is why the values of D_e, E_e do not vary greatly for the different cases analyzed and to a lesser extent the values of D_c, E_c cannot vary greatly because their values come mainly from the $S = 2$ state measurements.

D_e and E_e are a sum of contributions from the point dipole interaction and the exchange interaction. It is easily shown that $D_{dipole} = -3g^2\beta^2/R_{12}^3$ and $E_{dipole} = 0$, where R_{12} is the distance between the metal ions, which we know from the crystal structures. Values obtained for $D_{exchange}$ and $E_{exchange}$ are also given in Table 5. For the edta complex $D_{exchange}$ is 1.40 or -1.15 cm^{-1}, depending on the sign of D_e, and for the phen complex $D_{exchange}$ is 1.56 or -1.32 cm^{-1}. The relationship of D_c and E_c to the D and E values for individual metal ions is more complex and will be considered below.

Attempts to estimate R_{12} from the EPR spectra of dimeric copper complexes (for which $D_c = E_c = 0$) have been made in the hopes that $D_{exchange}$ and $E_{exchange}$ would be small or zero. It was found, however, that the exchange contribution to D and E in binuclear copper compounds was surprisingly large even if the value of J_{12} was as low as 30 cm^{-1}. The exchange contribution to ZFS is thought to be a synergic effect of both spin−orbit coupling on each ion and the exchange interactions between the ground state of one ion with the excited (electronic) states of the other ion. Magnitudes of the exchange integrals involved in these interactions (in particular $J(x^2 - y^2, xy)$) have been determined for copper[30] and vanadium[31] binuclear complexes. Ferromagnetic coupling was found, as expected, and the J_{12} values were of the order of hundreds of wavenumbers. The model used has been critized by Gribnau and Keijzers.[32] If we were to try to extend the theory used to explain the J anisotropy in these copper dimers to the high-spin iron(III) dimers studied here, we would predict a near-zero contribution to the ZFS from the exchange contribution. An important term in the theory is the same term that gives rise to the large anisotropy in the **g** matrix and its sizable deviation from the free-spin value, but for high-spin iron(III) the **g** matrix is nearly isotropic and close to the free-spin value.

Also in Table 5 are given the two calculated values of D and E predicted for the triplet ($S = 1$) state from eqs 6 and 7 or eq 10. $D(S = 1)$ is indeed very large in magnitude, as we deduced from our studies. If we could determine the spin-Hamiltonian of the triplet state, we could reduce the number of possible values listed in Table 5, but the one triplet line seen for the phen system did not give us sufficient information to allow a choice. Q-band powder spectra of the phen complex were obtained at a variety of temperatures below room temperature (see Figure 6) and do show evidence at the lower temperatures, where populations of quintet and septet states are very low, of the triplet spectrum, but the magnetic field range was not sufficient to make a determination of the magnitude for D. The large noise in the spectra is likely due to crystallite sizes in the powder not being small enough. Attempts to predict the EPR spectra for these large values have shown us that we could expect to detect an $S = 1$ resonance in the high-field region of our magnet when $|E|$ is less than 0.4−0.5 cm^{-1}, and therefore the smaller value of E in case 4 for the edta complex might be rejected since we detected no $S = 1$ transitions in this complex. The lower magnitudes found for the phen complex are consistent with the fact that we did detect an $S = 1$ transition for this compound. It should be pointed out that the large values of α_S

(30) Boillot, M. L.; Journaux, Y.; Bencini, A.; Gatteschi, D.; Kahn, O. *Inorg. Chem.* **1985**, *24*, 263 and references therein.
(31) Ozarowski, A.; Reinen, D. *Inorg. Chem.* **1986**, *25*, 1704.
(32) Gribnau, M. C. M.; Keijzers, C. P. *Inorg. Chem.* **1987**, *26*, 3413.

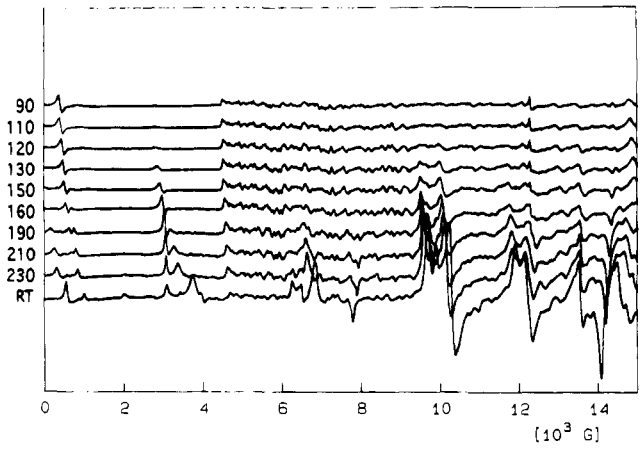

Figure 6. Powder Q-band EPR spectra of $\{[Fe(phen)_2]_2O\}(NO_3)_4 \cdot 7H_2O$ at temperatures (kelvin scale) indicated.

and β_S for $S = 1$ result in large errors in the predicted value of $E(S = 1)$. Single-crystal magnetic susceptibility studies[12a] on $[(Fe(salen)]_2O \cdot CH_2Cl_2$ have given a value for $D(S = 1)$ of 2 cm^{-1}. If we were confident that this is the sort of magnitude to be expected for $D(S = 1)$ in Fe−O−Fe, then case 2 for edta and case 1 for phen, which give the predicted $D(S = 1)$ values of 3.0 cm^{-1} for edta and 2.3 cm^{-1} for phen, are more likely. These cases also give the smaller magnitudes for the values of D_c which we will argue below are the more likely. All of these arguments are tenuous, and clearly EPR studies at higher frequencies or X-band studies at higher magnetic fields are needed. A discussion of the reliability of the theory used above to predict the spin-Hamiltonian parameters of $S = 1$ transitions will follow in the Discussion.

Analysis of D_c and E_c. It is of interest to see if one can extract from D_c and E_c an estimate of D_{loc} and E_{loc} for a single iron(III) ion if the other iron(III) ion in the dimer were not present. To do this, we will modify an approach used by Owen[29] which was for linear dimers. We have assumed the two local sites to be identical except for the orientations of their local principal axes which were assumed to be as shown in Figure 5. In this figure, we have shown the local principal z axis to be along the Fe−O bond axis, as it seems a reasonable first guess, but in fact we could choose α to be different from half the bond angle, in which case we would be assuming a C_{2v} symmetry for the dimer, which requires one principal axis to be perpendicular to the Fe−O−Fe plane and two axes in the plane. The assumptions made here make these equations applicable only to the phen system, in which the principal axes for both the D_c, E_c and D_e, E_e matrices are the same. After appropriate coordinate transformations, the following equations were obtained:

$$D_c = 0.5D_{loc}[3 \sin^2 \alpha - 1] + 1.5E_{loc} \cos^2 \alpha \quad (11)$$

$$E_c = 0.5D_{loc} \cos^2 \alpha + 0.5E_{loc}[1 + \sin^2 \alpha] \quad (12)$$

Using eqs 11 and 12, we obtain possible sets of values for (D_{loc}, E_{loc}) of (±1.275, ∓0.092) and (∓1.902, ±0.019) cm^{-1} using the values for D_c and E_c in Table 5. Experimentally, D values for high-spin iron(III) complexes[33-36] with similar ligands are in the range 0.6−1.0 cm^{-1}, which leads us to suggest that the experimental D and E values of the dimer leading to the lower D_{loc} values are probably more reasonable values.

Discussion

The main significance of this work is (1) it is the first complete analysis of the EPR spectra of two FeOFe dimers of high-spin iron(III) and (2) by detecting and characterizing two spin states of the dimer, we were able to separate, for the first time, the exchange contribution to the zero field from the contribution from distortions in the local ligand field for a dimer with two $S = 5/2$ ions. The large magnitude of $|D_{exchange}|$ (>1 cm^{-1}) cannot be accounted for by the theories put forward to explain the values of $D_{exchange}$ in dimers with $S = 1/2$, indicating a serious need for further consideration being given to the theory of the anisotropy of the exchange parameter J_{12}.

It is of interest to note that the distortion axis for the anisotropy in the exchange interaction is parallel to the Fe−Fe axis, and the small magnitude of E tells us there is little anisotropy in the exchange interaction about this axis. The bent Fe−O−Fe bond apparently has little influence on the anisotropy in J_{12}.

It should also be noted that, considering the magnitude of both D_c and D_e found in this work, we were able to detect both the $S = 2$ and $S = 3$ states only because these terms were of the same sign. If they were of opposite signs, all of the ZFS parameters would make detection at X-band very difficult due to their large magnitudes. This might explain why they have not been detected in some other Fe(III) dimer systems.

Okamura and Hoffman[10] have made an incomplete crystal EPR study of a closely related system, $enH_2[Fe(hedta)]_2 \cdot 6H_2O$, and reported for the $S = 2$ state a value of $D = |0.15|$ cm^{-1} with the principal distortion axis being the Fe−Fe direction. They also reported that the D value for the $S = 1$ state was too large to be analyzed, even at Q-band. Their value is quite consistent with our results although their value is only half the magnitude that we report for the $S = 2$ state of the edta complex. Remember, the measured D is the difference between D_e and D_c, which are an order of magnitude larger. In our edta complex the difference in the two terms in the Fe−Fe direction is the same magnitude as E_c, resulting in the principal distortion axis for the $S = 2$ state not being along the Fe−Fe direction even though that is the main distortion direction for the two matrices that are being subtracted from each other. If we were to reduce the E_c values obtained here for the edta complex to zero without changing anything else, we would predict a D value close to that reported by Okamura and Hoffman.[10] Thus the difference can be accounted for by small differences in the crystal field effects at each iron site.

It is important to extend this study to spectrometers with either higher frequencies or larger fields to detect and measure the spin-Hamiltonian for the triplet ($S = 1$) state. This is important not only to determine which set of possible parameters is correct but also to confirm the validity of the theory used to effect the separation of the exchange contribution from the local ligand field contribution. The exchange-coupled dimers have always been treated in the literature by a theory that is represented by eqs 1 and 6−9. This theory assumes that the energies of all spin states can be determined by one parameter: J_{12}. We know that this approximation must break down for large enough interactions between the two metal ions, but it is not certain how large is large enough. In eqs 6−9 it is assumed that the zero-order splitting of a given spin state can be accounted for by only two parameters, D_e and D_c. (It is also assumed that D_e and D_c are small compared to J_{12}, which in our case is a reasonable assumption.) Determination of the ZFS parameters

(33) Aasa, R. *J. Chem. Phys.* **1970**, *52*, 3919.
(34) Lang, G.; Aasa, R.; Garrelt, K.; Williams, R. J. P. *J. Chem. Phys.* **1971**, *55*, 4539.
(35) Cotton, S. A. *Chem. Phys. Lett.* **1976**, *41*, 606.
(36) Migita, C. T.; Ogura, K.; Yoshino, T. J. *Chem. Soc., Dalton Trans.* **1985**, 1077.

from three different spin states would allow us to check how well a two-parameter theory works. Kremer[37] has determined D for the $S = 1$, 2, and 3 states for two different crystals of a linear chromium(III) dimer. The three D values approximate the behavior predicted by eqs 6−9, but the deviations are considerably outside experimental error. For example, the $D(S = 1)$ values predicted from $D(S = 2)$ and $D(S = 3)$ are smaller than the experimental value by 0.4−0.5 cm^{-1}, which is 4 times the expected error. If one assumes D_e is fixed, D_c for $S = 1$ would have to be 10%−20% larger than that for the $S = 3$ state to fit the experimental results. Such a variation in our system would lead to a change in magnitude for $D(S = 1)$ of over 1 cm^{-1} due to the large value of β_1. We expect the assumption in the theory that one can treat the contribution of the local ligand fields to the ZFS as an additive property is questionable when there is such a large interaction between the two metal ions. It is probably better to assume that D_c will depend slightly upon S. We are, presently, exploring how we might determine the ZFS parameters for the $S = 1$ state in another laboratory.

Acknowledgment. This work was supported by operating grants (to B.R.M. and J.E.D.) from the Natural Sciences and Engineering Research Council of Canada. Powder EPR spectra at 34, 3.9, and 2.4 GHz were recorded by Dr. Ralph Weber, Bruker Instruments, Billerica, MA.

Supporting Information Available: Tables SI and SII, listing anisotropic thermal parameters for non-hydrogen atoms and final fractional coordinates and thermal parameters for hydrogen atoms (2 pages). Ordering information is given on any current masthead page. Structure factor tables may be obtained directly from the authors.

IC9503500

(37) Kremer, S. *Inorg. Chem.* **1985**, *24*, 887.